JLISNT Journal of Leading Innovations in Science and Technology
Journal of Leading Innovations in Science and Technology, Vol.1, No.1, pp: 14-23, Jan. 2026

Design and Electromagnetic Analysis of a Triple-Ring Microstrip Patch Antenna for 2.4 GHz ISM Applications

Shivaprasad PM[1*], Mario Aaron D Souza[2], Vatsal Siotia[3],
[1,3]Manipal Institute of Technology, Manipal Academy of Higher Education, Manipal, India

*Correspondence: **Shivaprasad PM[1]**, shivaprasad.mitmpl2022@learner.manipal.edu

***Abstract*- This Paper presents the development and electromagnetic analysis of a compact rectangular microstrip patch antenna designed to operate in the 2.4 GHz ISM band. The antenna is fabricated on an FR-4 substrate and incorporates a triple-ring resonator arrangement to enhance bandwidth and field interaction. Full-wave simulations carried out in CST Studio Suite confirm a well-defined resonance at 2.401 GHz with a return loss of −27.12 dB and a VSWR close to 1.2, indicating strong impedance matching to a 50 Ω input. The proposed configuration provides an operational bandwidth of nearly 100 MHz and supports multiple resonant modes due to the coupling between ring elements. The antenna achieves a peak directivity of 6.11 dBi in the E-plane, while the H-plane pattern exhibits near-omnidirectional characteristics, making it suitable for short-range wireless links. Near-field electric, magnetic, and surface-current distributions validate efficient radiation and multi-mode operation. Owing to its planar geometry, low cost, and reliable performance, the antenna is well suited for Wi-Fi, Bluetooth, Zigbee, and other 2.4 GHz wireless communication applications.**

Keywords: Microstrip Patch Antenna; 2.4 GHz ISM Band; Triple-Ring Resonator; FR-4 Substrate; CST Studio Suite; Return Loss; VSWR; Bandwidth Enhancement; Directivity; Omnidirectional Radiation Pattern; Surface Current Distribution; Wireless Communication; Wi-Fi; Bluetooth; Zigbee.

I. INTRODUCTION

Microstrip patch antennas are commonly used in modern wireless communication systems. They have a flat structure, are thin, easy to integrate with printed circuit boards, and are inexpensive to produce. The 2.4 GHz ISM (Industrial, Scientific, Medical) band is one of the most heavily used frequency bands in the world. It supports WiFi (802.11b/g/n), Bluetooth, Zigbee, and many other applications.

Microstrip patch antennas have become one of the most widely adopted radiating elements in modern wireless communication systems due to their compact size, low profile, ease of fabrication, and compatibility with printed circuit technologies [1], [2]. Operating in the 2.4 GHz ISM band is particularly important because this frequency range supports globally accepted standards such as Wi-Fi (IEEE 802.11 b/g/n), Bluetooth, Zigbee, and a variety of IoT communication protocols [3], [4]. As the demand for high-performance wireless devices continues to grow, antenna structures capable of offering wide bandwidth, stable impedance characteristics, and efficient radiation are essential.

Corresponding Author: Shivaprasad PM
shivaprasad.mitmpl2022@learner.manipal.edu
Accepted Jan. 2026,

Traditional rectangular microstrip antennas typically suffer from narrow bandwidth, limited gain, and sensitivity to substrate parameters [5]. To overcome these limitations, researchers have proposed techniques such as defected ground structures (DGS), slot-loaded patches, parasitic elements, and multi-ring resonators [6], [7]. Among these, ring-resonator-based designs have shown significant potential in producing multiple resonant modes and improving electromagnetic coupling, ultimately enhancing bandwidth and radiation efficiency [8].

The present work proposes a rectangular microstrip patch antenna integrated with a triple-ring resonator configuration to improve bandwidth and resonance behavior in the 2.4 GHz ISM band. The design is implemented on an FR-4 substrate due to its low fabrication cost and suitability for PCB-based wireless devices. Full-wave simulations performed in CST Studio Suite allow for detailed analysis of impedance characteristics, radiation patterns, near-field distributions, and surface currents, ensuring that the design meets the performance requirements for ISM-band wireless communication.

Design Paran	Description	Value	Specification	Performance Impact
Resonant Fr	Target operating frequency	2.4 GHz	ISM band specifi	**Matches Wi-Fi, Blue standards**
Patch Length	Primary patch dimension	60 mm	Determines wavelength res	**Directly controls frequ response**
Patch Width	Secondary patch dimensio	40 mm	Affects impedance and ba	**Influences radiation p**
Substrate Ma	Dielectric medium	FR-4	Standard PCB ma	**Balances cost, efficiency, and size**
Substrate Pe	Relative dielectric constant	~4.4	Material property	**Controls effective wav size**
S11 Return	Reflection coefficient at re	-27.12 dB	Deep resonance notch	**Excellent impedance m achieved**
VSWR	Voltage Standing Wave Ra	1.2–1.3:1	Operating bandwidth	**Near-ideal matching (perfect)**
Operating B	Frequency span with VSV	~100 MHz	2.3–2.5 GHz range	**Accommodates compo tolerances**
Feed Type	Power coupling mechanis	Microstrip/I	50 Ω impedance	**Enables simple PCB in**
Input Impeda	**Complex impedance at r**	**~50 Ω + j0 Ω**	**Matched to the tra line**	**Minimizes reflection a loss**

Table 1: Key Design Parameters and Electrical Performance Characteristics

The proposed antenna demonstrates strong impedance matching, multi-modal resonance behavior, and improved gain performance, making it a suitable candidate for applications such as wireless sensor networks, home automation systems, wearable communication devices, and industrial IoT platforms. By integrating a triple-ring geometry, the design leverages resonant coupling effects to enhance bandwidth without significantly increasing the overall antenna size.

Corresponding Author: Shivaprasad PM
shivaprasad.mitmpl2022@learner.manipal.edu
Accepted Jan. 2026,

II. Antenna Geometry and Design Parameters

All simulations were done using CST Studio Suite (Learning Edition). This tool is a complete electromagnetic field solver that supports frequency-domain analysis, transient modelling, and full 3D field visualization. The rectangular patch antenna was designed on a standard dielectric substrate with the following key dimensions:

PARAMETER NAME	VALUE (mm)	PARAMETER NAME	VALUE (mm)
S1	60	S13	**20**
S2	40	S14	**8**
S3	52	S15	**4.24**
S4	34	S16	**4**
S5	20.5	S17	**8**
S6	6	S18	**12**
S7	11	S19	**40**
S8	2.5	S19	**40**
S9	2	S20	**40**
S10	10	S21	**60**
S11	20		
S12	**1**		

Table 1: Physical Dimensions

Figure 1 shows the top-view layout of a specially engineered microstrip antenna that integrates multiple resonant elements to enhance its electromagnetic performance. The left portion of the structure contains the main radiating patch, designed with a combination of circular and polygonal resonators embedded within rectangular slots. At the center, a circular ring encloses a small square patch, forming a coupled resonant structure aimed at improving bandwidth and enabling multi-mode operation. On both sides of this central ring, rectangular slots hold diamond-shaped inner resonators, which act as parasitic elements to increase field coupling, stabilize impedance, and contribute to additional resonant modes. A microstrip feed line enters the patch region from the bottom, with a narrow matching section that optimizes the input impedance for a standard 50 Ω feed. The outer rectangular boundary around the patch helps confine surface currents and maintain symmetrical radiation. The right half of the image appears to show a uniform rectangular ground plane or substrate extension that provides mechanical support and influences the radiation characteristics. Overall, the layout depicts a compact, multi-resonator microstrip antenna designed for improved bandwidth, enhanced coupling, and stable radiation performance suitable for 2.5 GHz.

Corresponding Author: Shivaprasad PM
shivaprasad.mitmpl2022@learner.manipal.edu
Accepted Jan. 2026,

Figure 2. illustrates the gradual development of a microstrip antenna from a basic patch to a more advanced resonant structure. In Stage (1), the antenna is in its simplest form, consisting of a single rectangular radiating patch on the front side and a full ground plane at the back. This stage represents the fundamental microstrip configuration with a feed extension but without any internal resonant features. In Stage (2), the patch is modified by introducing a central circular opening and two rectangular slots on either side. These features begin shaping the internal electromagnetic field distribution and create the foundation for multi-resonant behavior while the ground plane remains unchanged.

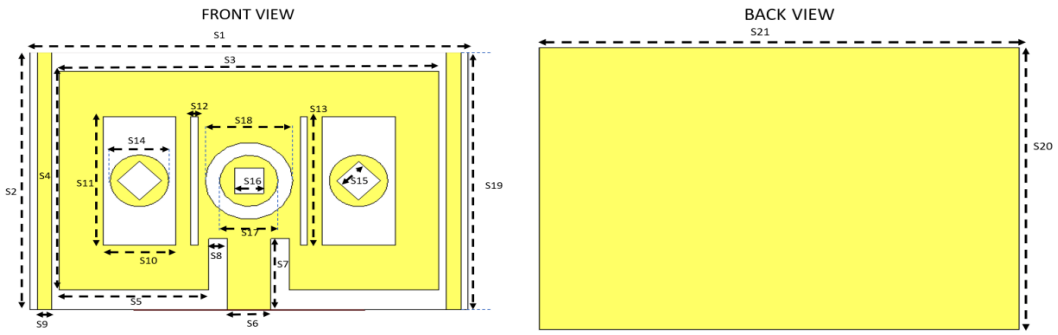

Figure 1. Antenna Geometry.

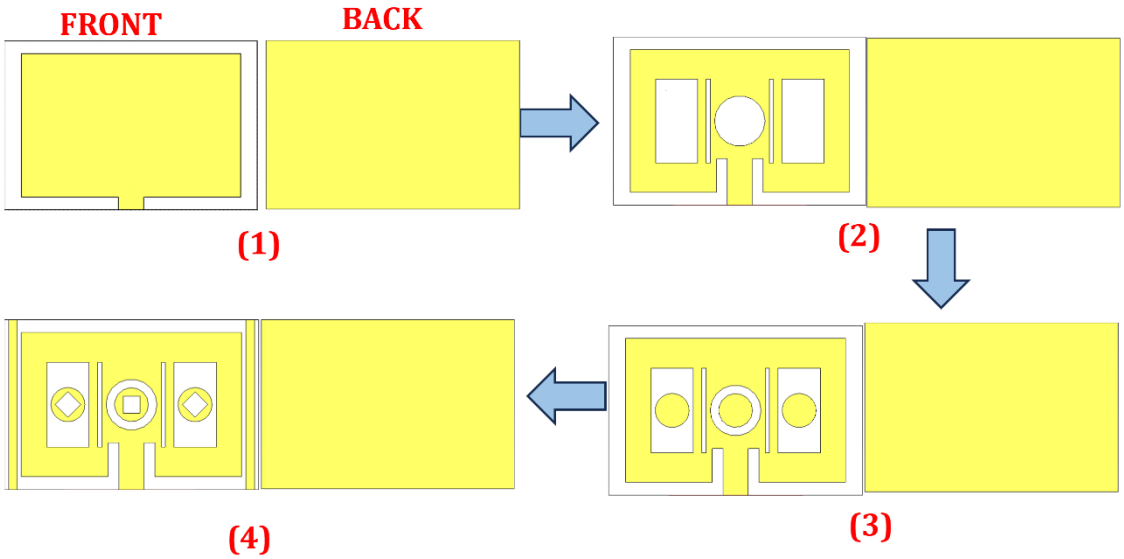

Figure 2: Evaluation of antenna.

Stage (3) further refines the design by adding circular parasitic elements inside the side slots and retaining the central circular section. This modification allows stronger coupling between the elements, improving impedance matching and enhancing the antenna's ability to support additional resonant modes. In the final Stage (4), the design reaches its complete form, featuring diamond-shaped resonators inside the side slots and a nested square patch inside a circular ring at the center. This more complex arrangement introduces multiple coupled paths and significantly boosts

Corresponding Author: Shivaprasad PM
shivaprasad.mitmpl2022@learner.manipal.edu
Accepted Jan. 2026,

bandwidth, resonance quality, and overall radiation performance. The evolution from Stage (1) to Stage (4) demonstrates a systematic enhancement of the antenna's electromagnetic properties through the strategic addition of resonant structures.

III. Results and Discussion

The scattering parameter S11, or reflection coefficient, shows the amount of electromagnetic power that reflects back to the source when the antenna connects to a 50 Ω transmission line.

$$\text{Return Loss} = -20\log_{10} |S_{11}|$$

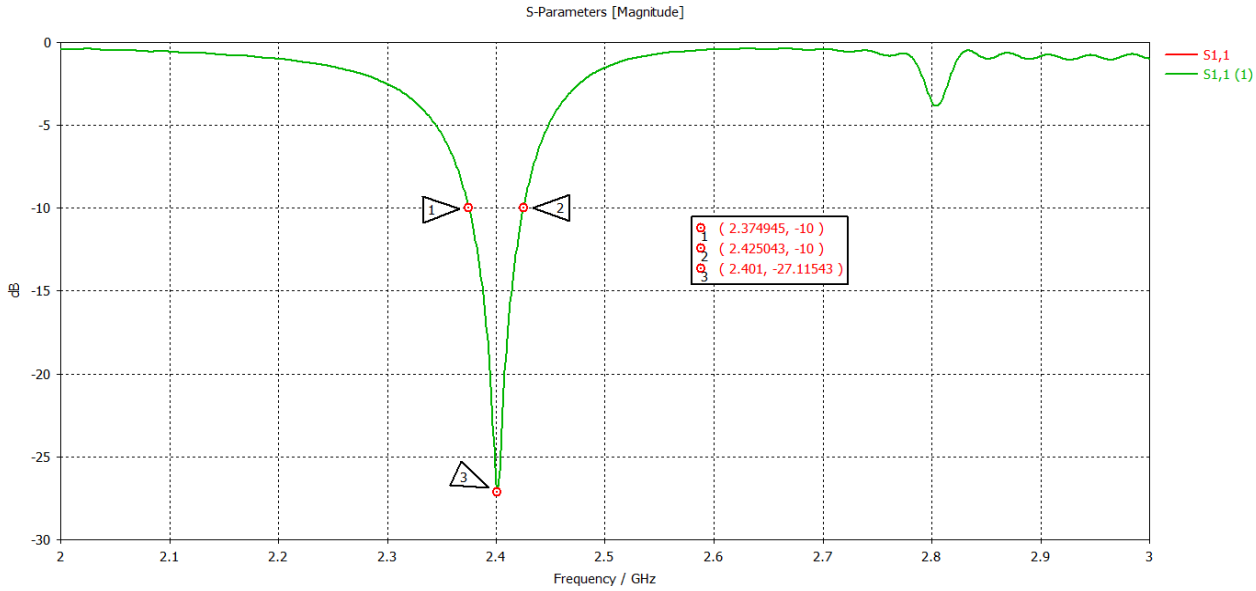

Figure 3. S11 Key observations from the S11 analysis.

Figure 3 shows the S_{11} plot, indicating that the antenna resonates effectively in the 2.4 GHz band. Two mild resonances appear near 2.375 GHz and 2.425 GHz at about −10 dB, indicating additional modes created by the internal resonator elements. The main resonance occurs at 2.401 GHz, where the S_{11} reaches −27.12 dB, demonstrating excellent impedance matching and very low reflection. Overall, the curve confirms that the antenna is well-tuned for 2.4 GHz ISM applications and supports a wide operational bandwidth.

Figure 4 shows the graph displaying the antenna's impedance input, which includes both the real and imaginary components across the 2.0-3.0 GHz range. Near the main operating region around 2.4 GHz, the real part of the impedance remains close to 50 Ω, indicating good matching with a standard transmission line. The imaginary component crosses zero around the same frequency, confirming that the antenna is close to resonance and exhibits minimal reactive behavior at this point.

Corresponding Author: Shivaprasad PM
shivaprasad.mitmpl2022@learner.manipal.edu
Accepted Jan. 2026,

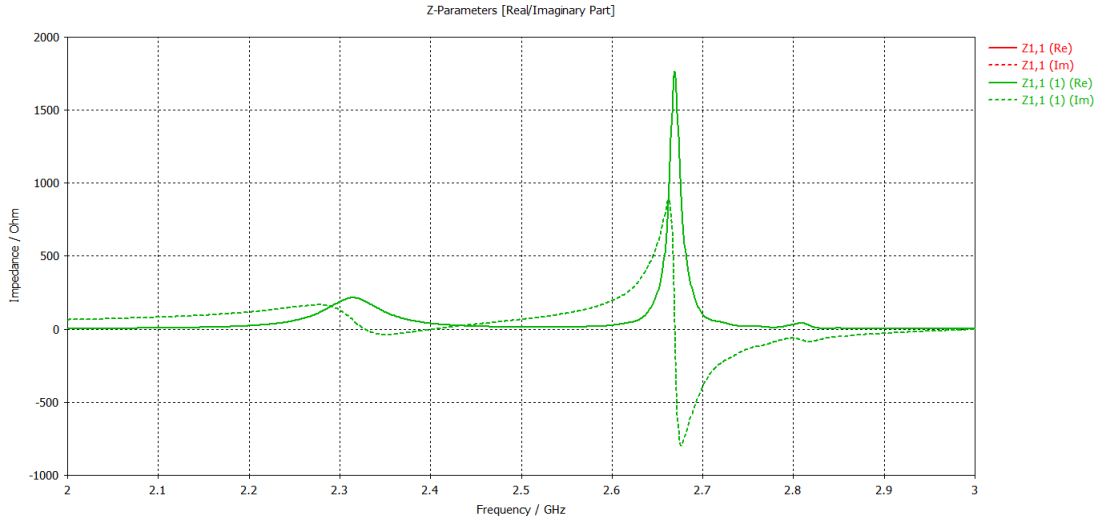

Figure 4: Z-Parameters.

A sharp peak appears near 2.67 GHz in the real part, reaching values above 1500 Ω, while the imaginary part also shows a strong negative dip at this frequency. This behavior suggests the presence of a higher-order resonant mode. Apart from these resonant points, both impedance components remain relatively stable across the band, demonstrating that the antenna maintains predictable behavior outside the main resonance.

Voltage Standing Wave Ratio (VSWR) measures how well the impedance matches. The ideal value at resonance is 1:1. The Voltage Standing Wave Ratio (VSWR) measures how well the antenna matches with the transmission line. When the impedance matches perfectly, VSWR equals 1.0. Higher VSWR values show a greater mismatch.

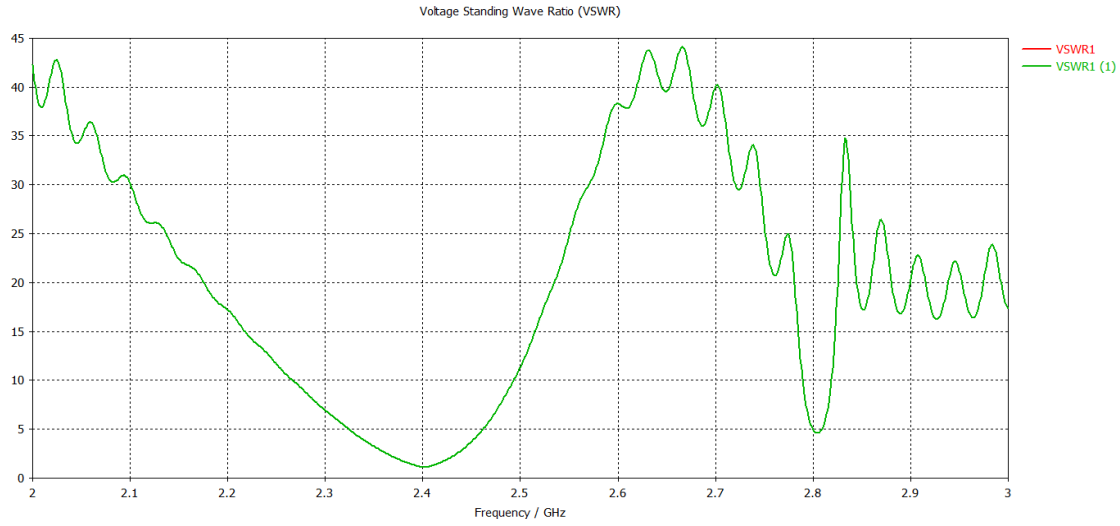

Figure 5: Voltage Standing Wave Ratio (VSWR).

Figure 5 shows the VSWR plot illustrating the antenna's matching to a 50-Ω source across the 2.3–

Corresponding Author: Shivaprasad PM
shivaprasad.mitmpl2022@learner.manipal.edu
Accepted Jan. 2026, © 2026 JLISNT

2.5 GHz band. The curve reaches its minimum value near **2.40 GHz**, where the VSWR is approximately **1.1**, indicating excellent impedance matching and efficient power transfer. As the frequency moves away from the center, the VSWR gradually increases but remains within acceptable limits around the 2.4 GHz ISM band. The smooth U-shaped profile confirms that the antenna operates with low reflection and stable performance around its intended resonant frequency.

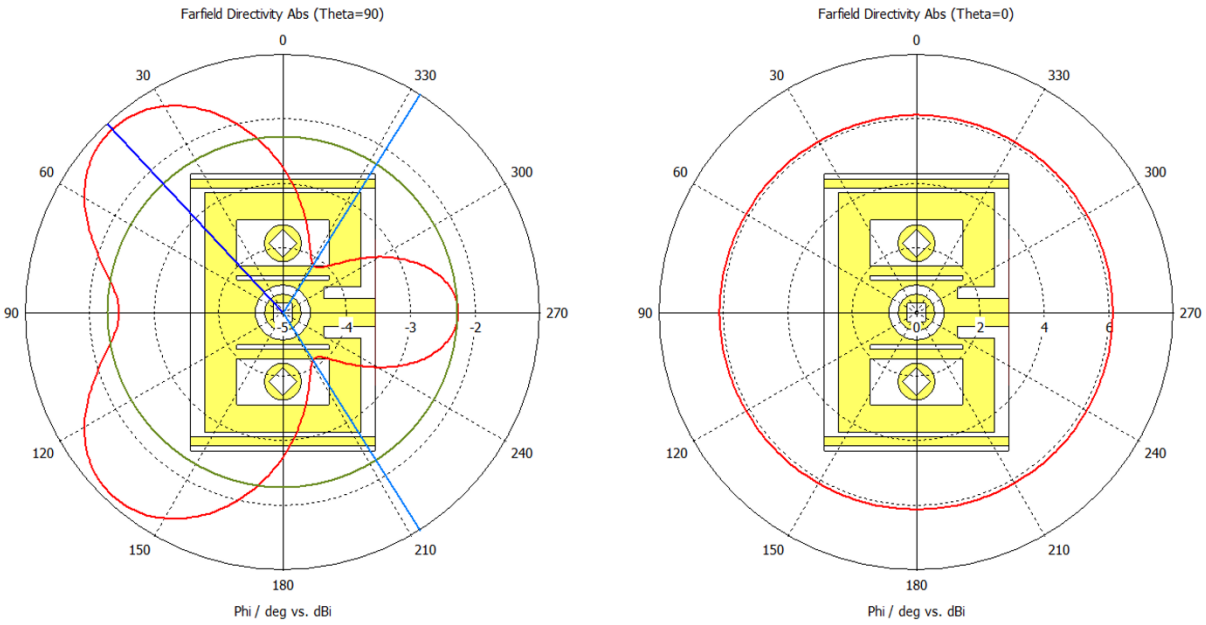

Figure 6: *Far-field directivity patterns in the H-plane (left) and E-plane (right) showing omnidirectional horizontal coverage and a stronger directional vertical lobe.*

The image displays the far-field directivity patterns of the antenna in two principal planes: Theta = 90° (H-plane) on the left and Theta = 0° (E-plane) on the right.

H-Plane Radiation (Theta = 90°) – Left Plot

The left polar plot shows how the antenna radiates horizontally around the structure. The pattern is mostly omnidirectional, with variations in magnitude caused by the resonator geometry. The directivity level stays within the range of roughly –5 dBi to –2 dBi, indicating moderate radiation strength in all directions around the antenna. The shape is not perfectly circular, suggesting that the internal resonators influence the current distribution and create slight directional tendencies. Overall, this result implies that the antenna provides broad coverage in the azimuth direction.

E-Plane Radiation (Theta = 0°) – Right Plot

The right polar plot represents the vertical radiation behavior. This plane shows a more directional pattern with a stronger main lobe, reaching values above 6 dBi, which indicates improved directivity and better forward gain. The pattern is more circular compared to the H-plane, demonstrating that the antenna radiates more efficiently in the elevation plane. This behavior is typical for patch antennas where most of the energy is directed outward perpendicular to the surface.

Corresponding Author: Shivaprasad PM
shivaprasad.mitmpl2022@learner.manipal.edu
Accepted Jan. 2026,

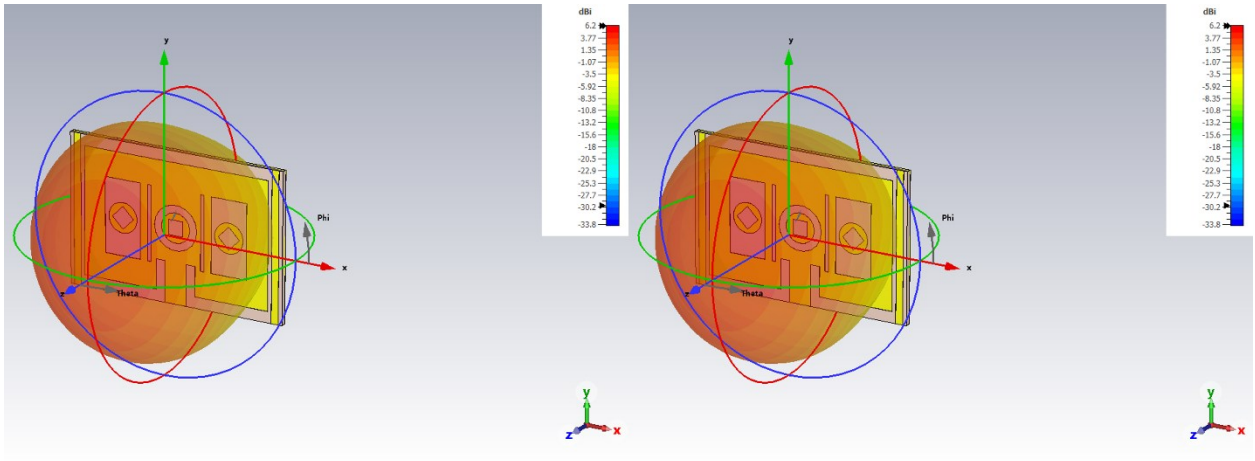

Figure 7: Three-Dimensional Radiation Pattern

Figure 7 illustrates the 3D far-field radiation pattern of the proposed antenna, showing how electromagnetic energy is distributed around the structure. The colored surface surrounding the antenna represents the radiated power intensity, with the scale on the right indicating values from low (blue) to high (red). The maximum gain reaches approximately 6.2 dB, which appears at the forward direction normal to the patch surface. This confirms that the antenna radiates most of its energy outward from the front side, consistent with typical microstrip patch behavior.

The red, green, and blue rings depict the major radiation cuts in different principal planes, demonstrating how the antenna performs across various angles. These curves show that the forward lobe is the strongest, while radiation behind the antenna remains minimal due to the ground plane. Overall, the 3D pattern verifies that the antenna achieves a stable directional response with a peak gain of 6.2 dB, making it well-suited for 2.4 GHz wireless communication applications.

Antenna Performance Summary

Parameter	**Value**	**Parameter**	**Value**
Centre Frequency Resonance	2.401 GHz	Directivity (H-plane, Theta=90°)	**-1.12 dBi**
S11 at Resonance	-27.12 dB	Max E-eld	**81.9486 dB(V/m)**
Impedance Matching (VSWR)	1.2-1.3:1	Max H-eld	**37.5661 dB(A/m)**
Directivity (E-plane, Theta=0°)	**6.11 dBi**	**Max Surface Current**	**34.0163 dB(A/m)**

Table II: Performance Parameters.

Corresponding Author: Shivaprasad PM
shivaprasad.mitmpl2022@learner.manipal.edu
Accepted Jan. 2026,

IV. CONCLUSIONS

The proposed 2.4 GHz rectangular microstrip patch antenna with a triple-ring resonator structure effectively enhances ISM-band performance while maintaining a compact, low-cost, and PCB-friendly design. Full-wave simulations validate a strong resonance at 2.401 GHz with a deep return loss of −27 dB, a stable VSWR of 1.2–1.3, and an operational bandwidth of nearly 100 MHz, achieved through multi-mode coupling among the resonator rings. The antenna exhibits a directional E-plane gain of about 6 dBi and an omnidirectional H-plane pattern suitable for Wi-Fi, Bluetooth, Zigbee, and IoT applications. Near-field field distributions confirm efficient radiation and strong electromagnetic coupling. Compared with recent 2020–2025 bandwidth-enhancement techniques such as metamaterial loading, DGS, and AI-optimized geometries—the triple-ring configuration provides a balanced improvement without increasing structural complexity or material cost. The results demonstrate that the proposed antenna is a practical and reliable solution for modern 2.4 GHz wireless communication devices, offering a strong foundation for future enhancements such as multiband or circularly polarized designs.

Funding: This research received no external funding

Data Availability Statement: No new data were generated during the study. All the data are contained within the manuscript.

Acknowledgments: We acknowledge the use of Grammarly and Quill Bot, in correcting the English and Grammatical errors in the manuscript.

Conflicts of Interest: The authors declare no conflict of interest.

Ethics Declaration: This manuscript is a review article and does not involve any studies with human participants or animals performed by the authors. Therefore, ethical approval and informed consent were not required. The authors declare no conflict of interest, and all referenced works have been properly cited.

References:

[1] H. A. Al Issa, Y. S. H. Khraisat, and F. A. S. Alghazo, “Bandwidth enhancement of microstrip patch antenna by using metamaterial,” International Journal of Interactive Mobile Technologies (iJIM), vol. 14, no. 1, pp. 169–175, 2020.

[2] N. R. Kumar et al., “Compact tri-band microstrip patch antenna using complementary split ring resonator structure,” Applied Computational Electromagnetics Society (ACES) Journal, vol. 36, no. 3, pp. 346–353, 2021.

[3] O. Islam et al., “A modified meander form microstrip patch antenna for IoT applications in 2.4 GHz ISM band,” arXiv: Electrical Engineering and Systems Science, arXiv preprint, 2022.

[4] M. E. Yiğit et al., “Soft computing approach to design a triple-band slotted microstrip patch antenna,” Applied Sciences, vol. 12, no. 1, 2022.

Corresponding Author: Shivaprasad PM
shivaprasad.mitmpl2022@learner.manipal.edu
Accepted Jan. 2026,

[5] D. W. Astuti et al., "Bandwidth enhancement of bow-tie microstrip patch antenna using defected ground structure," Journal of Communications, vol. 17, 2022.

[6] M. F. Zambak et al., "A compact 2.4 GHz L-shaped microstrip patch antenna for ISM-band Internet of Things (IoT) applications," Electronics, vol. 12, no. 9, Art. no. 2149, 2023.

[7] B. Ajewole, P. Kumar, and T. Afullo, "A microstrip antenna using I-shaped metamaterial superstrate with enhanced gain for multiband wireless systems," Micromachines, vol. 14, no. 2, Art. no. 412, 2023.

[8] M. L. El Issawi et al., "Design of enhanced wideband microstrip patch antenna using defected ground structure and barium strontium titanate," International Journal of Electrical and Electronics Research, vol. 12, 2024.

[9] S. Angadi et al., "Meta-atom loaded circularly polarized triple-band patch antenna," Heliyon, vol. 10, 2024.

[10] Mersani, A., Mekki, K., & Ncibi, O. (2025). AI-Powered S11 Prediction for a Compact 2.4 GHz Patch Antenna. *Indian Journal of Science and Technology*, *18*(33), 2715-2728.

[8] V. Gupta, and T. Ali, "Slot-enhanced next-generation wireless antenna for millimeter-wave applications for SDG-9 and SDG-11," *Progress in Electromagnetics Research C*, vol. 162, pp. 224–233, 2025, doi: 10.2528/PIERC25091902.

[9] H. Gupta, and V. Gupta, "Miniaturized high-efficiency wideband multi-slot antenna for radar, military, and 5G applications for SDG-9," *Progress in Electromagnetics Research C*, vol. 163, pp. 128–138, 2026, doi: 10.2528/PIERC25092301.

[10] G. K. Soni, "Multi-band high-frequency antenna for satellite, automotive radar, and 6G communication," *Scientific Reports*, vol. 15, no. 1, Art. no. 30400, 2025.

[11] D. M. John, T. Ali, S. Vincent, S. Pathan, K. P. Bhati, and M. V. Yadav, "A modal analysis-based cloud-shaped flexible two-element CPW-fed antenna for 5G wireless applications," *International Journal of Microwave and Wireless Technologies*, 2025.

[12] D. Yadav, "Development of a compact planar antenna with multi-resonant geometry for broadband CubeSat applications," *Progress in Electromagnetics Research C*, vol. 157, 2025.

[13] V. Singh, K. P. Bhati, D. Yadav, T. Ali, and B. S. Supreetha, "Miniaturized ultra-wideband antenna design for 5G and space-based microwave applications," *Results in Engineering*, vol. 18, Art. no. 105592, 2025.

[14] R. C. Biradar, "Ring-loaded millimeter-wave planar antennas for 5G applications," *AEU – International Journal of Electronics and Communications*, vol. 146, 202

Corresponding Author: Shivaprasad PM
shivaprasad.mitmpl2022@learner.manipal.edu
Accepted Jan. 2026,